Extremophiles (2009) 13:875–884
DOI 10.1007/s00792-009-0275-x

ORIGINAL PAPER

Molecular cloning and stress-dependent expression of a gene encoding Δ^{12}-fatty acid desaturase in the Antarctic microalga *Chlorella vulgaris* NJ-7

Yandu Lu · Xiaoyuan Chi · Qingli Yang · Zhaoxin Li · Shaofang Liu · Qinhua Gan · Song Qin

Received: 5 June 2009 / Accepted: 3 August 2009 / Published online: 1 September 2009

Abstract The psychrotrophic Antarctic alga, *Chlorella vulgaris* NJ-7, grows under an extreme environment of low temperature and high salinity. In an effort to better understand the correlation between fatty acid metabolism and acclimation to Antarctic environment, we analyzed its fatty acid compositions. An extremely high amount of Δ^{12} unsaturated fatty acids was identified which prompted us to speculate about the involvement of Δ^{12} fatty acid desaturase in the process of acclimation. A full-length cDNA sequence, designated CvFAD2, was isolated from *C. vulgaris* NJ-7 via reverse transcription polymerase chain reaction (RT-PCR) and RACE methods. Sequence alignment and phylogenetic analysis showed that the gene was homologous to known microsomal Δ^{12}-FADs with the conserved histidine motifs. Heterologous expression in yeast was used to confirm the regioselectivity and the function of CvFAD2. Linoleic acid (18:2), normally not present in wild-type yeast cells, was detected in transformants of CvFAD2. The induction of CvFAD2 at an mRNA level under cold stress and high salinity is detected by real-time PCR. The results showed that both temperature and salinity motivated the upregulation of CvFAD2 expression. The accumulation of CvFAD2 increased 2.2-fold at 15°C and 3.9-fold at 4°C compared to the alga at 25°C. Meanwhile a 1.7- and 8.5-fold increase at 3 and 6% NaCl was detected. These data suggest that CvFAD2 is the enzyme responsible for the Δ^{12} fatty acids desaturation involved in the adaption to cold and high salinity for Antarctic *C. vugaris* NJ-7.

Keywords Cold stress · High salinity stress · Antarctic · Δ^{12} fatty acid desaturases

Abbreviations
UFA Unsaturated fatty acid
FAD Fatty acid desaturases

Introduction

Chlorella vulgaris NJ-7 was isolated from an algal mat residing on the surface of a rock nearby the Zhongshan Station (China) of Antarctica where the temperature was

Y. Lu and X. Chi are co-first authors.

Communicated by T. Matsunaga.

Y. Lu · S. Qin (✉)
Yantai Institute of Coastal Zone Research for Sustainable Development, Chinese Academy of Sciences, 264003 Yantai, People's Republic of China
e-mail: sqin@ms.qdio.ac.cn

Y. Lu · S. Liu
Institute of Oceanology, Chinese Academy of Sciences, 266071 Qingdao, People's Republic of China
e-mail: luyandu@webmail.hzau.edu.cn

Y. Lu · S. Liu
Graduate School of the Chinese Academy of Sciences, 100049 Beijing, People's Republic of China

X. Chi · Q. Yang
Shandong Peanut Research Institute, 266100 Qingdao, People's Republic of China

Z. Li
Yellow Sea Fisheries Research Institute, Chinese Academy of Fishery Sciences, 266071 Qingdao, People's Republic of China

Q. Gan
Shandong Entry-Exit Inspection and Quarantine Bureau, 266001 Qingdao, People's Republic of China

almost 9.9°C in the summer and can fall to −45.7°C in severe winters, a range of 55°C. Compared with other well studied cold-adapted chlorophytes that failed to grow at temperatures above 20°C (Morgan-Kiss et al. 2005, 2008), *C. vulgaris* NJ-7 grow well at temperature between 4 and 30°C (Hu et al. 2008). Thus, this newly isolated photopsychrotrophile has retained a higher versatility in response to environmental change.

Cold-adapted organisms are evidently adapted to the extreme environmental conditions found within the ice and have evolved a number of adaptive mechanisms to counteract the effects of temperature change (Stefanidi and Vorgias 2008). But more importantly, they are able to acclimate rapidly to the changing physicochemical conditions within the brine channel systems. Even small temperature changes of 1–2°C greatly influence the structure of these microhabitats as well as the chemical and physical properties of the ice. Furthermore, organisms that inhabit the interstices and underside of sea ice are exposed to wide variations of salinity, particularly during the periods of brine drainage and ice melting. The capability of responding to rapid changes in a host of external stresses, including temperature and salinity, is therefore an intrinsic characteristic of life in sea ice and just as important as being able to survive freezing temperatures (Mock and Thomas 2005). *C. vulgaris* NJ-7 would make the first candidate for the research on the mechanism of wide acclimation to dramatically changing habitat.

In this study, we analyzed the fatty acid composition of *C. vulgaris* NJ-7. The extremely high rate of Δ^{12} unsaturated fatty acids (UFAs) allowed us to isolate a Δ^{12} desaturase. The function of CvFAD2 was determined by expression in *Saccharomyces cerevisiae*, in particular, the effects of temperature and salinity on the expression profile of CvFAD2 were investigated. The results provide new insights for the acclimation of organisms to low temperature and high salinity.

Materials and methods

Strains and growth condition

C. vulgaris NJ-7 was presented from Pro. Xu Xudong (Institute of Hydrobiology, Chinese Academy of Sciences). The green alga was grown in batch cultures in a salt medium (BG11) (Stanier et al. 1971), and initially maintained at a temperature of 25°C with 12 h of incandescent light and 12 h of darkness.

Fatty acid analysis

As a first step in defining the acclimation to changing Antarctic ambience, we analyzed the fatty acids composition of *C. vugaris* NJ-7. Algae were cultivated to logarithmic phase at 25°C, and then some algae were harvested. Others were divided into five treatments: 25°C, 0% (w/v) NaCl (control); 15°C, 0% NaCl; 4°C, 0% NaCl; 25°C, 3% NaCl; 25°C, 6% NaCl. After an interval of 36 h, algae were harvested and the total lipids were extracted and analyzed according to the method described by Hsiao et al. (2007).

Nucleic acid manipulation

C. vulgaris NJ-7 in exponential growth phase were harvested by centrifugation at 5000 rpm for 5 min at 4°C and washed with sterile, distilled, deionized water to remove salts before they were centrifuged again. The dried mass was frozen in liquid nitrogen, ground with mortar and pestled into a fine powder. Total RNA was extracted from the powder according to the method of Li (Li et al. 2008b). The RNA samples were used for RACE and real-time PCR after DNaseI treatment to remove DNA. The first-strand cDNA was synthesized with RT-PCR kit (Qiagen) according to the manufacturer's instructions. 500 ng of total RNA was used in a 20 μl reaction system. Controls received water instead of reverse transcriptase to assess any contamination from genomic DNA as described by Zhou et al. (2007).

PCR with degenerate primers

First-strand cDNA was used as a template for PCR. Available sequences of Δ^{12}-acyl-lipid desaturases from the GenBank database (Benson et al. 2005) were used to design two degenerate primers, F1/R1 (Table 1). F1 and R1 were corresponding to the highly conserved regions HRRHHSN and DTHVAHH.

PCR contained 1× PCR Ex-Taq buffer (Mg^{2+} plus), 0.2 mM of each dNTP, 0.4 μM of each primer, and 1 U of Ex-Taq (Takara) per 25 μl reaction. Amplifications run on a Tpersonal Thermocycler 118 (Biometra, Germany) using the following parameters: an initial 5 min denaturation step at 94°C, followed by 30 cycles of 94°C for 30 s, 56°C for 30 s, and 72°C for 1 min, finally extended at 72°C for 7 min. The PCR fragments were cloned into pMD-18-T vector (Takara) and sequenced.

Full-length cDNA and genomic sequences isolation

The nucleotide sequences of the 3′ and 5′-ends of CvFAD2 were amplified by the RACE method (Sambrook et al. 2001). Amplifications were carried out using the SMART RACE cDNA Amplification Kit (BD-Clontech) according to the manual. 3′ and 5′ RACE were performed using gene-specific primers (3GSP1, 3GSP2, 5GSP1 and

Table 1 Primers used in experiment

Aim	Oligonucleotide sequence 5′–3′	Product size (bp)
Partial cDNA cloning		
F1	CAYCGNCGBCACCAYTCCAACAC	542
R1	TGGTGNGCNACRTGHGTGTC	
5′ RACE		
5GSP1	CCAACGCCACGTCACTGATT	517
5GSP2	GCCAGAGACCCAGTGTTGGA	
3′ RACE		
3GSP1	CACACACACCCAGAGCTGCC	1068
3GSP2	CTACGGCTGGCTGCTCAACA	
Full-length cDNA and genomic sequences cloning		
F2	GGGAATCACCAAGAGCCTGTCAAGA	1251
R2	AGCATCTTTCCATCGCCGAGAACA	
F3	CACCAAGCGTTCAGCGAGAG	1522
R3	GTGATTGTGACGAGCCAGAA	
F4	ACTTCTGGCTCGTCACAATC	2254
R4	TAGGAGAAGCGAGGAAGCAA	
Real-time PCR		
F5	GCTTCCAAGGGCAAACTCAGG	127
R5	GAGACGGGTCACAACACAAAAAAG	
F6	ACATCCGCAAGGACCTGTACTC	163
R6	CCGATCCACACGCTGTACTTG	
pYFAD2 construction		
F7	*GAATTC*AAG***ATG***GTGCAAACCCGCCGCCAGT	1161
R7	*CTCGAG****TCA***CTTTCTGAACCAGTAGATGCC	

F forward, *R* reverse

5GSP2, Table 1). PCR was carried out using the formulation described in the manual. The program was performed as follows: 5 min at 94°C, followed by 30 s at 94°C, 3 min at 72°C, for 5 cycles, 30 s at 94°C, 30 s at 70°C and 3 min at 72°C, for 5 cycles, 30 s at 94°C, 30 s at 68°C and 3 min at 72°C, for 25 cycles, finally extended at 72°C for 7 min. Nested PCR was carried out using the nested universal primers and gene-specific primers. Secondary PCR fragments were subcloned into pMD-18-T vector and nucleotide sequences were determined subsequently.

Based on the information of 3′ and 5′-ends sequences, two gene-specific primers F2 and R2 (Table 1) were designed to amplify full-length cDNA. PCR was performed with the GC-Rich PCR system (Takara) using 1× GC buffer (Mg^{2+} plus) 0.2 mM dNTP, 0.5 μM F2 and R2, 1 U of LA-Taq per 25 μl reaction. Reaction conditions were as follows: 5 min denaturation at 94°C, followed by 30 cycles of 94°C for 30 s, 58°C for 30 s and 72°C for 90 s, finally extended at 72°C for 7 min. The PCR fragments of the expected length (1.2 kb) was cloned into pMD-18-T vector and sequenced. For genomic sequence cloning, two sets of primers were designed and named as F3, R3, F4 and R4 (Table 1). An overlapping region was obtained for the splicing of the whole genomic sequence.

Sequence analysis

Sequence analysis was carried out according to the method of Li (Li et al. 2008a). A BLAST search program (http://www.ncbi.nlm.nih.gov/blast/) was used. Multiple sequence alignment of putative CvFAD2 was performed with Clustalx1.81 (Thompson et al. 1997). The distribution of the hydrophobic amino acids was analyzed using Kyte–Doolittle hydropathy scale (http://www.expasy.ch/cgi-bin/protscale.pl) (Kyte and Doolittle 1982). Transmembrane (TM) regions of the protein were predicted with transmembrane hidden Markov model (TMHMM) (http://www.cbs.dtu.dk/services/TMHMM/) (Moller et al. 2001). The signal sequence analysis was done using a signal peptide prediction server (http://www.cbs.dtu.dk/services/SignalP-3.0/) (Bendtsen et al. 2004).

Phylogenetic affiliation of the CvFAD2 was examined by comparing it to the confirmed and putative plastidial and microsomal Δ^{12} fatty acid desaturases (FAD) obtained from public database. Amino acid sequences were aligned using ClustalX program with the implanted BioEdit (Chenna et al. 2003; Thompson et al. 1997). Phylogenetic trees were constructed using neighbor-joining methods, as implemented in the program MEGA4 (Tamura et al. 2007). Minimum evolution and maximum parsimony analyses

were also performed. Bootstrap support was estimated using 1000 replicates for distance analyses. Default program parameters were used.

Quantification real-time PCR

For real-time PCR, algae were cultivated to logarithmic phase at 25°C, and were then divided into five treatments: 25°C, 0% (w/v) NaCl (control); 15°C, 0% NaCl; 4°C, 0% NaCl; 25°C, 3% NaCl; 25°C, 6% NaCl. After an interval of 36 h, algae were harvested.

Two pairs of gene-specific primers (Table 1) were designed according to the CvFAD2 cDNA (F5 and R5) and β-actin sequences (F6 and R6). Standard curves for CvFAD2 and β-actin genes were generated by tenfold serial dilutions (10^5–10^{10} copies/μl) of each plasmid DNA. PCR products were quantified continuously with ABI 7900 Real-Time PCR System (Applied Biosystems) using SYBR Green fluorescence (Takara) according to the manufacturer's instructions. Control reactions were amplified with RNA template but without reverse transcriptase. The relative amounts of CvFAD2 RNA were normalized to the respective β-actin transcripts. The $2^{-\triangle\triangle CT}$ method (Livak and Schmittgen 2001) was used to analyze quantitative real-time PCR data.

Expression in *S. cerevisiae*

Two specific primers were used to obtain the full-length open reading frames. F7 and R7 (Table 1) corresponds to the nucleotide sequences of start and stop codons (in bold face), respectively. The 5′ end of the F7 and R7 contains an *Eco*RI or an *Xho*I restriction site (italicized) to facilitate subsequent manipulation. The amplified cDNA was digested and subcloned into the *Eco*RI–*Xho*I site of the expression vector pYES2.0 (Invitrogen) to generate a plasmid designated pYFAD2. The sequence orientation and identity were confirmed by sequencing. *S. cerevisiae* INVSc1 was transformed and selected according to the manual.

Heterologous expression of CvFAD2 was induced under transcriptional control of the yeast GAL1 promoter. Yeast cultures were grown to logarithmic phase at 30°C in synthetic minimal medium (SC-Ura). The cells were induced as described by Robert et al. (2009). Cultures were incubated at 15°C for a further 48 h prior to harvesting. The cells were harvested by centrifugation, and washed three times with sterile distilled water and then dried by lyophilization. The total lipids were extracted and analyzed according to the method described by Hsiao et al. (2007).

Nucleotide sequencing and accession number

The nucleotide sequences of CvFAD2 genomic and cDNA have been deposited and assigned accession number GQ175318 and EU596474 in the EMBL/GenBank/DDBJ database.

Results

Fatty acid distribution

The amount of 18:2 and 18:3 UFAs were 33.08 and 24.99% in *C. vulgaris* NJ-7 (Table 2). On the other side, they were 5.88 and 21.59% in *Chlamydomonas raudensis* Ettl (UWO241) and 19.25 and 11.50% in *Chlorella* BI, respectively (Morgan-Kiss et al. 2008). The total amount of the Δ^{12} UFAs of *C. vulgaris* NJ-7 (58.07%) is 2.11- and 1.89-fold compared with *C. raudensis* Ettl (UWO241) and *Chlorella* BI, respectively.

The major composition was 16:0 which shared half of fatty acids in *Chlorella* BI. On the other hand, the main components were 14:0 and 18:3 in *C. raudensis* and their amounts were closely equal to each other. Although all three microalgae were Antarctic, the difference of fatty

Table 2 Comparision of fatty acid distribution of *C. vulgaris* NJ-7, *C. raudensis* and *Chlorella* BI

Fatty acid	Fatty acid distribution (percent of total by mass)		
	C. vulgaris NJ-7	*Chlorella* BI (Morgan-Kiss et al. 2008)	*C. raudensis* (Morgan-Kiss et al. 2008)
14:0	0.39	3.48	25.86
16:0	16.33	49.88	11.15
18:0	1.31	0.54	0.63
16:1	4.95	5.18	11.09
16:2	8.66	2.01	2.91
16:3	6.97	1.77	7.11
18:1	0.41	5.88	6.39
18:2	33.08	19.25	5.88
18:3	24.99	11.50	21.59

Table 3 Comparision of fatty acid distribution of *C. vulgaris* NJ-7 at different temperature or salt concentration

Fatty acid	Fatty acid distribution (percent of total by mass)				
	25°C	15°C	4°C	3% NaCl	6% NaCl
16:2	7.37 ± 0.6	7.40 ± 0.1	8.63 ± 0.6	7.53 ± 0.4	7.77 ± 0.2
16:3	11.65 ± 1.9	10.58 ± 0.7	10.39 ± 2.5	8.17 ± 0.3	9.95 ± 1.1
18:2	28.51 ± 2.1	30.21 ± 3.6	31.01 ± 3.1	29.89 ± 0.1	29.48 ± 4.5
18:3	28.86 ± 1.5	28.34 ± 8.8	27.01 ± 5.6	26.94 ± 3.6	26.33 ± 1.0
16:2 and 18:2	35.88 ± 1.5	37.62 ± 3.5	39.64 ± 3.6	37.42 ± 0.3	37.25 ± 4.2
Δ^{12}	76.39 ± 4.5	76.54 ± 12.7	77.04 ± 6.93	72.53 ± 3.0	73.53 ± 3.7

Data are presented as the mean ± SD ($n = 3$)

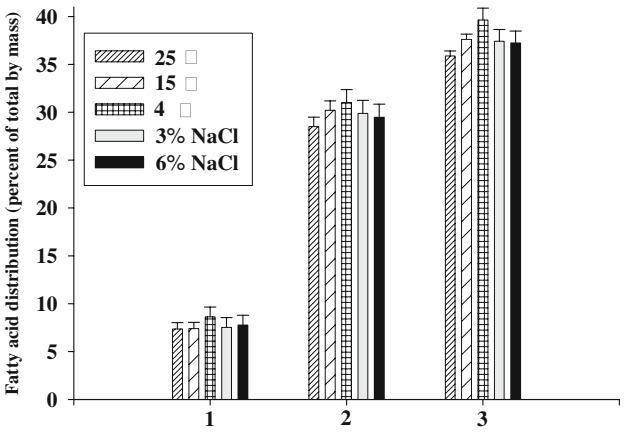

Fig. 1 Comparisons of fatty acid distributions of *C. vulgaris* NJ-7 at different temperature or salt concentration. *1* 16:2, *2* 18:2, *3* 16:2 + 18:2

acid composition was impressive. A question must be explicitly addressed here in understanding of the role of lipids in fine tuning membrane function. At low temperatures, a more fluid membrane can usually be attained by increasing the degree of fatty acid unsaturation or branching and by decreasing the fatty acid chain length (Feller 2007). These low melting-point fatty acids lower the gel–liquid crystalline-phase transition temperature of the lipid and therefore maintain proper fluidity at low temperatures. For the sake of maintaining fluidity of the membrane, different strategies were adopted. The strategy for *C. vulgaris* NJ-7 is primarily to increase the content of straight-chain UFAs. In contrast, the strategy for *Chlorella* BI appears to be mainly dependent upon increasing the amount of short chain fatty acids. *C. raudensis* may regulate membrane fluidity by both strategies.

Fatty acid distributions under different treatments were studied in order to know the linkage between fatty acids alteration and stresses. Total amount of Δ^{12} fatty acids (16:2, 16:3, 18:2, 18:3) increased at lower temperature. On the other hand, less Δ^{12} fatty acids were observed in *C. vulgaris* NJ-7 at 3 and 6% NaCl (Table 3). However, 18:2 and 16:2 increased in response to exposure to lower temperature and higher salinity (Fig. 1).

Based on these observations, we tentatively put forward that Δ^{12} UFAs were important players in the rapid acclimation of *C. vulgaris* NJ-7 to the Antarctic environment. Thus, a research on its Δ^{12} FADs expression profile will help to illuminate the mechanism of the process.

cDNA and genomic DNA sequences identification

A 542 bp cDNA fragment was generated by RT-PCR with degenerate primers. The fragment shared a 73% sequence similarity to Δ^{12} FAD genes from *Chlorella* C-27 and 57% to *Chlamydomonas reinhardtii*. It indicated a partial putative FAD2 was isolated from Antarctic *C. vulgaris* NJ-7. Gene-specific primers were further designed to obtain the full-length CvFAD2. A 517 bp 5′-RACE product and a 1068 bp 3′-RACE product were amplified. The nucleotide sequences of both products from RACE experiments shared an identical 35 and 60 bp sequence overlap on flanking regions of the partial putative CvFAD2 cDNA fragment, suggesting that these fragments are portions of the same gene. Sequence analysis revealed that the cloned CvFAD2 cDNA was 2032 bp in length, which contained a 1158 bp open reading frame, a 50 bp 5′-untranslated region, and a 824 bp 3′-untranslated region with the characteristics of the poly (A) tail. An ATG translation initiation codon was identified in the sequence of the 5′ terminus (51–53 bp), and a TAA termination codon was found 1158 bp downstream of the initiation site.

To elucidate the genomic organization, the genomic DNA sequence of CvFAD2 was cloned and aligned with cDNA sequence. The result indicated that CvFAD2 consisted of eight exons. The sizes of the exons and introns are summarized in (Table 4). Seven are canonical GT/AG splicing signals at the ends of the putative introns. However, the sixth intron does not conform to that pattern. Rare splice donor consensus (GC) had been found, instead of (GT) after exon ending at position 2542. Spliceosomal introns generally begin with GT and end with AG dinucleotide motifs that are referred to as donor and acceptor

splice sites, respectively. However, introns with noncanonical splice sites have been identified in some organisms (Burset et al. 2000; Davis et al. 2000; Bon et al. 2003).

Comparison with other desaturases

CvFAD2 encoded 385 amino acid residues with an estimated molecular mass of 45.5 kDa and a theoretical isoelectric point of 6.87. A Blast search revealed that the primary structure of CvFAD2 showed high similarity to known microsomal Δ^{12} FAD, with a 75% identity to *Chlorella* C-27 (BAB78716, Suga et al. 2002), 57% to *C. reinhardtii* (XP_001691669), 53% to *Punica granatum* (AAO37754), 52% to *Jatropha curcas* (ABA41034) and 52% to *Arachis hypogaea* (AAY67653).

Table 4 Gene structures of *C. vulgaris* NJ-7 FAD2

Exon	Genomic start	Genomic end	Exon length
1	1	141	141
2	449	516	68
3	971	1093	123
4	1367	1545	179
5	2052	2158	107
6	2489	2542	54
7	2823	2920	98
8	3236	3754	520

Length and splicing positions are listed

The distribution of the hydrophobic amino acids of CvFAD2 was typical for a membrane protein, as identified using the Kyte–Doolittle hydropathy scale (Kyte and Doolittle 1982). The prediction of TM helices by TMHMM indicated that the deduced protein contained four hydrophobic domains between amino acids 54–76, 86–108, 178–200 and 250–272, which would be long enough to span the membrane bilayer twice, with the N-terminus facing the cytosol (Moller et al. 2001).

A multiple sequence alignment of CvFAD2 against similar Δ^{12} desaturase highlighted conserved motifs including HRRHHSN and DTHVAHH against which the degenerate primers were designed (Fig. 2). Otherwise three conserved histidine boxes, HXCGH (109–113) and HXXHH (145–149, 321–325), were found to be located in hydrophilic regions separated by long hydrophobic or membrane spanning regions. The histidine-rich motifs, highly conserved among membrane-bound acyl-CoA and

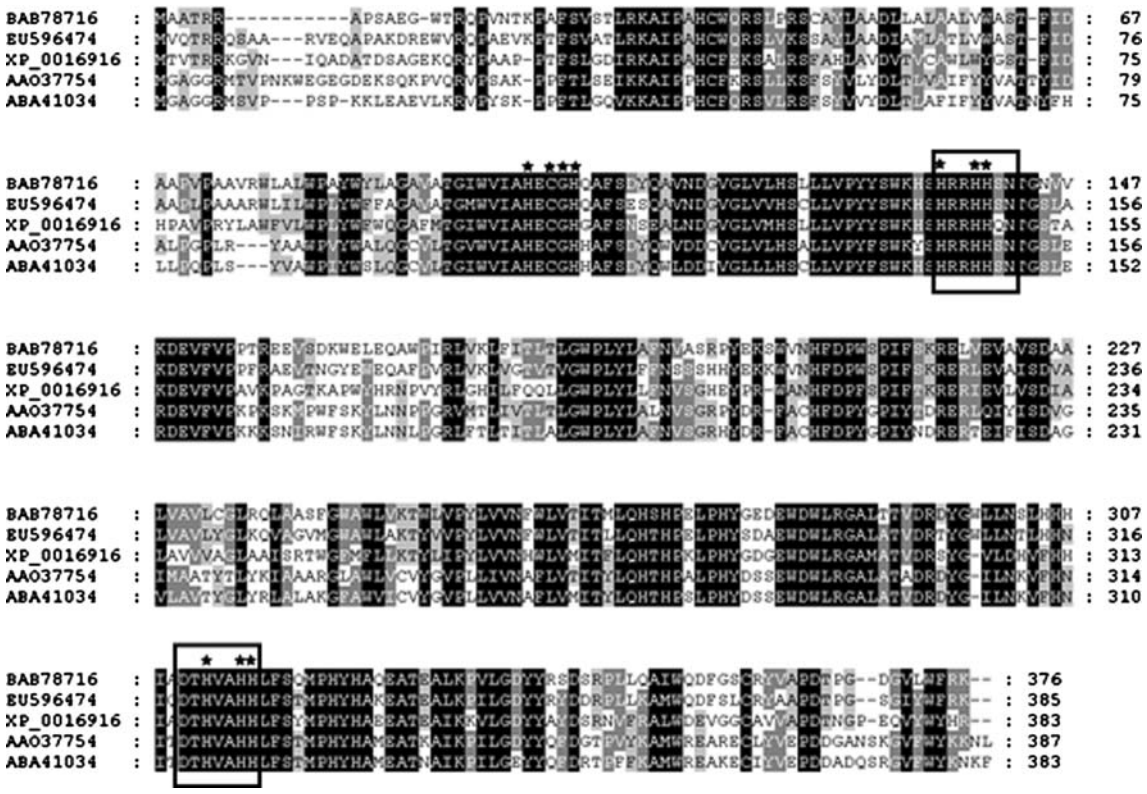

Fig. 2 Multiple alignments of amino acid sequences of *C. vulgaris* NJ-7 Δ^{12}-desaturase and other Δ^{12} desaturase. The deduced amino acid sequence of the *C. vulgaris* NJ-7 Δ^{12}-desaturase was subjected to BLAST analysis. The closest relatives were then selected and aligned using ClustalW. The conserved motifs HRRHHSN and DTHVAHH are highlighted in *boxes* and *asterisks* denote the histidine motifs. Sequences shown are Δ^{12} FADs: BAB78716 *Chlorell* C-27, EU596474-CvFAD2, XP_001691669 *C. reinhardtii*, AAO37754 *P. granatum*, ABA41034 *J. curcas*

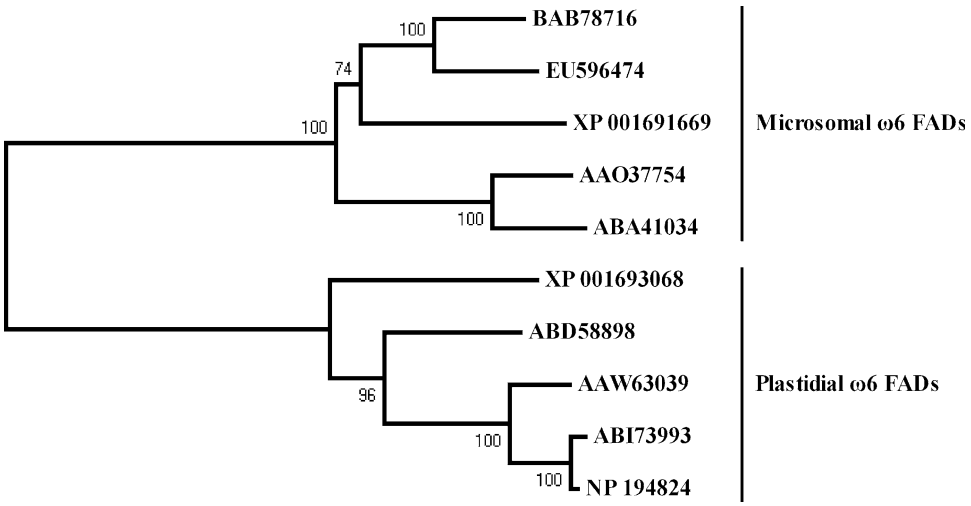

Fig. 3 Phylogenetic tree for Δ^{12} FAD and related desaturases based on amino acid sequences. Bootstrap analysis of 1000 randomized sequence replicates was performed. Sequences shown are: NP_194824 *Arabidopsis thaliana*, ABI73993 *Descurainia Sophia*, AAW63039 *Olea europaea*, ABD58898 *Mesostigma viride*, XP_001693068, XP_001691669 *C. reinhardtii*, ABA41034 *J. curcas*, AAO37754 *P. granatum*, EU596474-CvFAD2, BAB78716 *Chlorell* C-27

acyl-lipid desaturases, were proposed to form the potential diiron active site (Shanklin et al. 1994).

Phylogenetic analysis using deduced amino acid sequences of several other Δ^{12} FADs is shown (Fig. 3). All tree topologies are highly congruent. Two major clades are very well supported based on bootstrap values. All of the plastidial Δ^{12} FADs are grouped. CvFAD2 is clustered within microsomal Δ^{12} FAD group. Based upon its sequence similarity and phylogenetic analysis, it implies that CvFAD2 encodes a microsomal Δ^{12} FAD. Further evidence to support this proposal is that CvFAD2 has a truncated N-terminal (data not shown) whereas the plastidial Δ^{12} FADs have redundant N-terminals signal peptides for subcellular location predicted by hidden Markov models (Bendtsen et al. 2004).

Functional analysis in *S. cerevisiae*

Heterologous expression in yeast was used to confirm Δ^{12} regioselectivity and function of CvFAD2. Both pYFAD2 and empty vector, pYES2 (control), were transformed into the *S. cerevisiae* INVSc1. Total lipids of the transformants were put through GC–MS analysis. The results showed a novel fatty acid peak from pYFAD2, which was absent from the control (Table 5). The novel fatty acid was 18:2, by comparison of the retention time to FAME standard mixtures (Sigma). The result indicates that CvFAD2 encodes a Δ^{12}-FAD, which can convert 18:1 into 18:2 in yeast. This is consistent with the recent reports where Δ^{12}-FADs from the *Lentinula edodes* (Sakai and Kajiwara 2005) and *Rhizopus arrhizus* (Wei et al. 2004) recognize only one substrate (18:1) in yeast. Conversely, Δ^{12} FAD from *Phaeodactylum tricornutum* (Domergue et al. 2003), *Sapium sebiferum* (Niu et al. 2007) and *Chlorella* C-27 (Suga et al. 2002) were found to recognize two substrates (16:1 and 18:1) though 18:1 was the preferred substrate. It may indicate different TM topologies of these Δ^{12} FADs (Wei et al. 2004).

Table 5 Composition of the major fatty acids (% w/w) of pYES2 and pYFAD2 yeast transformants by GC–MS analysis

Transformant	16:0	16:1	16:2	18:0	18:1	18:2
pYES2	19.2	34.8	0	9.9	31.9	0
pYFAD2	24.3	36.0	0	9.2	27.0	1.6

Effects of temperature and salt stress on CvFAD2 expression

The gene expression patterns of CvFAD2 in Antarctic *C. vulgaris* NJ-7 were analyzed by quantification real-time PCR (qRT-PCR). β-actin was used as a reference for total RNA. β-actin PCR product was not detected when reverse transcriptase was omitted, indicating that the RNA template was free of genomic DNA. The data reveal that temperature and salt concentration regulate the accumulation of CvFAD2 mRNA. Transcripts accumulation increased 2.2- and 3.9-fold when the algae at 25°C were transferred to 15 or 4°C (Fig. 4a). It is different from plastidial Δ^{12} FAD (CvFAD6) which remained constantly when the algae at 25°C were transferred to 15°C (unpublished results). It signifies that they play different roles in temperature acclimation. Microsomal Δ^{12} FAD initiated transcripts accumulation in response to major or intermediate temperature shifts whereas plastidial one was only upregulated in response to major shifts. On the other hand, CvFAD2 was expressed abundantly under salt stress, 1.7-fold increase at 3% NaCl and 8.5-fold at 6% NaCl (Fig. 4b).

Discussion

The Antarctic *C. vugaris* NJ-7 grew well when exposed to wide variations of temperature compared with other characterized Antarctic microalgae (Hu et al. 2008; Morgan-Kiss

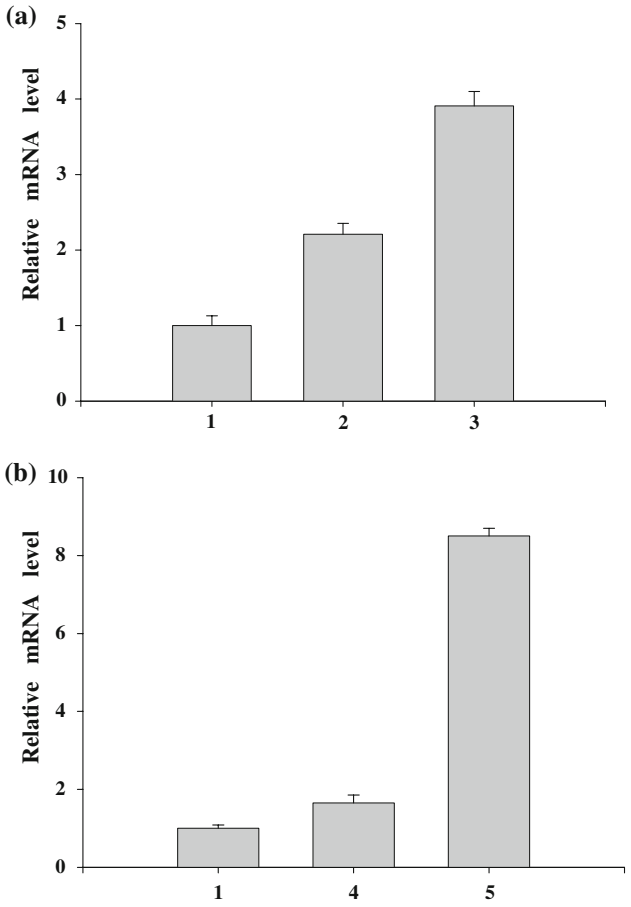

Fig. 4 Expression of CvFAD2 at different temperature **(a)** or salt concentration **(b)**. The qRT-PCRs were employed to quantify the relative amounts of CvFAD2 transcripts in 25°C (*1*), 15°C (*2*), 4°C (*3*), 3% NaCl (*4*) and 6% NaCl (*5*). Data are presented as the mean ± SD ($n = 3$)

et al. 2005, 2008). In order to realize the mechanism, we analyzed its fatty acid composition as the first step on account of the close correlation between fatty acid and temperature. As expected, *C. vugaris* NJ-7 overwhelmingly exceeds others in Δ^{12} UFAs constitution. Thus, we proposed that *C. vulgaris* NJ-7 take advantage of the increased content of straight-chain UFAs instead of short chain fatty acids to acclimate the extreme habitats. Therefore, Δ^{12} FAD may be an important player in the psychology modulation to counteract the effects of the cold. So we isolated CvFAD2 from *C. vulgaris* NJ-7 using RT-PCR with degenerate primers designed from conserved motifs and RACE method. The isolated protein was found to contain features characterizing Δ^{12} desaturases. It was grouped with the microsomal Δ^{12} desaturases according to the phylogenetic analysis. The function of CvFAD2 was validated by the expression in *S. cerevisiae*. 18:1 was utilized as precursor and converted to 18:2 by CvFAD2 in vivo. These results suggested that this gene encoded microsomal Δ^{12} FAD. CvFAD2 genomic organization suggested an alternative splicing since the rare splice sites (GC) in the sixth intron was found. The clarification to noncanonical splicing has the potential to facilitate accurate gene prediction further.

Based on the qRT-PCR analysis, the expression profile of CvFAD2 was characterized. Transcript was increased when the alga was transfer from 25 to 15°C or 4°C after 36 h. It was different from the cold response of CvFAD6 which remained a constant accumulation from 25 to 15°C (unpublished results). It suggested that CvFAD2 and CvFAD6 responded differently to changing temperature. CvFAD2 expression was activated in intermediate and major temperature shifts whereas CvFAD6 was only activated in major shifts. On the other hand, CvFAD2 also engaged in the adaption of high salinity stress. Changes in cellular membranes are adaptations to hypersalinity, that have been previously reported in yeasts (Turk et al. 2007; Gostincar et al. 2009), fungi (Turk et al. 2004, 2007) and cyanobacteria (Allakhverdiev et al. 2001). The restructuring of membrane lipid composition is one of the adaptations to high concentration of salt, which is mainly achieved by increasing the unsaturation of its phospholipid fatty acids. The possible reason was as that increase in unsaturation of fatty acids in membrane lipids significantly enhanced the tolerance of the photosynthetic machinery to salt stress. The enhanced tolerance was due both to the increased resistance of the photosynthetic machinery to the salt-induced damage and to the increased ability of cells to repair the photosynthetic and Na^+/H^+ antiport systems (Allakhverdiev et al. 2001).

Although temperature-dependent expression of FAD2 genes have been previously reported (Suga et al. 2002), to our knowledge, this is the first characterized FAD2 with the response to both low temperature and high salinity. It should be noted that this study has only examined the accumulation of CvFAD2 in transcription level, further study should be focus on the post-transcription and translation levels of global differentially expressed proteins, and stability of fatty acid biosynthesis genes to demonstrate the detailed involvement of FAD profiles in the process of acclimation. Nevertheless, this desaturase along with the recently characterized genes from the same organism represents an attractive biotechnological resource for development of an agricultural viable breed as highlighted in recent publications (Tran et al. 2009; Sengupta and Majumder 2009; Yokotani et al. 2009). In addition, it can be used for conferring high oleic acid profile on the seed oil and for producing high oleic plant lines. Further mining of the genome of Antarctic *Chlorella* NJ-7 should lead to identification of gene encoding these additional enzyme activities (de Pascale et al. 2008) and shed light on the acclimation of organisms to low temperature and high salinity.

Acknowledgments We thank Prof. Xu Xudong (Institute of Hydrobiology, Chinese Academy of Sciences) for providing the Antarctic microalga strain *C. vulgaris* NJ-7. This work was supported by the National High-Tech Research and Development Plan of China (No. 2006AA10A114), the National Key Basic Research and Development Project of China (No. 2007CB116212), the Key Innovative Project of Chinese Academy of Science (KSCX2-YW-G-002, KZCX2-YW-225), the National Natural Science Foundation of China (30670165, 40876082) and the Key Technology Research Project of Qingdao (No. 07-1-4-16-nsh).

References

Allakhverdiev SI, Kinoshita M, Kinoshita M, Inaba M, Suzuki I, Murata N (2001) Unsaturated fatty acids in membrane lipids protect the photosynthetic machinery against salt-induced damage in *Synechococcus*. Plant Physiol 125:1842–1853

Bendtsen JD, Nielsen H, von Heijne G, Brunak S (2004) Improved prediction of signal peptides: SignalP 3.0. J Mol Biol 340:783–795

Benson DA, Karsch-Mizrachi I, Lipman DJ, Ostell J, Wheeler DL (2005) GenBank. Nucleic Acids Res 33:D34–D38

Bon E et al (2003) Molecular evolution of eukaryotic genomes: hemiascomycetous yeast spliceosomal introns. Nucleic Acids Res 31:1121–1135

Burset M, Seledtsov IA, Solovyev VV (2000) Analysis of canonical and non-canonical splice sites in mammalian genomes. Nucleic Acids Res 28:4364–4375

Chenna R, Sugawara H, Koike T, Lopez R, Gibson TJ, Higgins DG, Thompson JD (2003) Multiple sequences alignment with the clustal series of programs. Nucleic Acids Res 31:3497–3500

Davis CA, Grate L, Spingola M, Ares M Jr (2000) Test of intron predictions reveals novel splice sites, alternatively spliced mRNAs and new introns in meiotically regulated genes of yeast. Nucleic Acids Res 28:1700–1706

de Pascale D, Cusano M, Autore F, Parrilli E, di Prisco G, Marino G, Tutino ML (2008) The cold-active Lip1 lipase from the Antarctic bacterium *Pseudoalteromonas haloplanktis* TAC125 is a member of a new bacterial lipolytic enzyme family. Extremophiles 12:311–323. doi:10.1007/s00792-008-0163-9

Domergue F, Spiekermann P, Lerchl J, Beckmann C, Kilian O, Kroth PG, Boland W, Zähringer U, Heinz E (2003) New insight into *Phaeodactylum tricornutum* fatty acid metabolism. Cloning and functional characterization of plastidial and microsomal Δ^{12}-fatty acid desaturases. Plant Physiol 131:1648–1660

Feller G (2007) Life at low temperatures: is disorder the driving force? Extremophiles 11:211–216. doi:10.1007/s00792-006-0050-1

Gostincar C, Turk M, Plemenitaš A, Gunde-Cimerman N (2009) The expressions of Δ^{9}-, Δ^{12}-desaturases and an elongase by the extremely halotolerant black yeast *Hortaea werneckii* are salt dependent. FEMS Yeast Res 9:247–256

Hsiao TY, Holmes B, Blanch HW (2007) Identification and functional analysis of a Δ-6 desaturase from the marine microalga *Glossomastix chrysoplasta*. Mar Biotechnol 9:154–165

Hu HH, Li HY, Xu XD (2008) Alternative cold response modes in *Chlorella* (Chlorophyta, Trebouxiophyceae) from Antarctica. Phycologia 47:28–34

Kyte J, Doolittle RF (1982) A simple method for displaying the hydropathic character of a protein. J Mol Biol 157:105–132

Li Y, Dietrich M, Schmid RD, He B, Ouyang P, Urlacher VB (2008a) Identification and functional expression of a Δ^{9}-fatty acid desaturase from *Psychrobacter urativorans* in *Escherichia coli*. Lipids 43:207–213

Li Y, Sommerfeld M, Chen F, Hu Q (2008b) Consumption of oxygen by astaxanthin biosynthesis: a protective mechanism against oxidative stress in *Haematococcus pluvialis* (Chlorophyceae). J Plant Physiol 165:1783–1797

Livak KJ, Schmittgen TD (2001) Analysis of relative gene expression data using real-time quantitative PCR and the $2^{-\triangle\triangle CT}$ method. Methods 25:402–408

Mock T, Thomas DN (2005) Recent advances in sea-ice microbiology. Environ Microbiol 7:605–619

Moller S, Croning MD, Apweiler R (2001) Evaluation of methods for the prediction of membrane spanning regions. Bioinformatics 17:646–653

Morgan-Kiss RM, Ivanov AG, Pocock T, Krol M, Gudynaite-Savitch L, Huner NPA (2005) The Antarctic psychrophile, *Chlamydomonas raudensis* Ettl (UWO241) (Chlorophyceae, Chlorophyta), exhibits a limited capacity to photoacclimate to red light. J Phycol 41:791–800

Morgan-Kiss RM, Ivanov AG, Modla S, Czymmek K, Huner NPA, Priscu JC, Lisle JT, Hanson TE (2008) Identity and physiology of a new psychrophilic eukaryotic green alga, *Chlorella* sp., strain BI, isolated from a transitory pond near Bratina Island, Antarctica. Extremophiles 12:701–711

Niu B, Ye H, Xu Y, Wang S, Chen P, Peng S, Ou Y, Tang L, Chen F (2007) Cloning and characterization of a novel Δ^{12}-fatty acid desaturase gene from the tree *Sapium sebiferum*. Biotechnol Lett 29:959–964

Robert SS, Petrie JR, Zhou XR, Mansour MP, Blackburn SI, Green AG, Singh SP, Nichols PD (2009) Isolation and characterisation of a Δ^{5}-fatty acid elongase from the marine microalga *Pavlova salina*. Mar Biotechnol 11:410–418. doi:10.1007/s10126-008-9157-y

Sakai H, Kajiwara S (2005) Cloning and functional characterization of a Δ^{12} fatty acid desaturase gene from the basidiomycete *Lentinula edodes*. Mol Genet Genomics 273:336–341

Sambrook J, Fritsch EF, Maniatis T et al (2001) Molecular cloning: a laboratory manual. Cold Spring Harbour Laboratory Press, New York

Sengupta S, Majumder AL (2009) Insight into the salt tolerance factors of a wild halophytic rice, *Porteresia coarctata*: a physiological and proteomic approach. Planta 229:911–929

Shanklin J, Whittle E, Fox BG (1994) Eight histidine residues are catalytically essential in a membrane-associated iron enzyme, stearoyl-CoA desaturase, and are conserved in alkane hydroxylase and xylene monooxygenase. Biochemistry 33:12787–12794

Stanier RY, Kunisawa R, Mandel M, Cohen-Bazire G (1971) Purification and properties of unicellular blue-green algae. Bacteriol Rev 35:171–205

Stefanidi E, Vorgias CE (2008) Molecular analysis of the gene encoding a new chitinase from the marine psychrophilic bacterium *Moritella marina* and biochemical characterization of the recombinant enzyme. Extremophiles 12:541–552. doi:10.1007/s00792-008-0155-9

Suga K, Honjoh K, Furuya N, Shimizu H, Nishi K, Shinohara F, Hirabaru Y, Maruyama I, Miyamoto T, Hatano S, Iio M (2002) Two low-temperature-inducible *Chlorella* genes for delta12 and omega-3 fatty acid desaturase (FAD): isolation of delta12 and omega-3 fad cDNA clones, expression of delta12 fad in *Saccharomyces cerevisiae*, and expression of omega-3 fad in *Nicotiana tabacum*. Biosci Biotechnol Biochem 66:1314–1327

Tamura K, Dudley J, Nei M, Kumar S (2007) MEGA4: molecular evolutionary genetics analysis (MEGA) software version 4.0. Mol Biol Evol 24:1596–1599

Thompson JD, Gibson TJ, Plewniak F, Jeanmougin F, Higgins DG (1997) The CLUSTAL_X windows interface: flexible strategies

for multiple sequence alignment aided by quality analysis tools. Nucleic Acids Res 25:4876–4882

Tran LS, Quach TN, Guttikonda SK, Aldrich DL, Kumar R, Neelakandan A, Valliyodan B, Nguyen HT (2009) Molecular characterization of stress-inducible *GmNAC* genes in soybean. Mol Genet Genomics. doi:10.1007/s00438-009-0436-8

Turk M, Mejanelle L, Šentjurc M, Grimalt JO, Gunde-Cimerman N, Plemenitaš A (2004) Salt-induced changes in lipid composition and membrane fluidity of halophilic yeast-like melanized fungi. Extremophiles 8:53–61

Turk M, Abramović Z, Plemenitaš A, Gunde-Cimerman N (2007) Salt stress and plasma-membrane fluidity in selected extremophilic yeasts and yeast-like fungi. FEMS Yeast Res 7:550–557

Wei DS, Li MC, Zhang XX, Ren Y, Xing LJ (2004) Identification and characterization of a novel Δ^{12}-fatty acid desaturase gene from *Rhizopus arrhizus*. FEBS Lett 573:45–50

Yokotani N, Ichikawa T, Kondou Y, Matsui M, Hirochika H, Iwabuchi M, Oda K (2009) Tolerance to various environmental stresses conferred by the salt-responsive rice gene *ONAC*063 in transgenic *Arabidopsis*. Planta 229:1065–1075. doi:10.1007/s00425-009-0895-5

Zhou XR, Robert SS, Petrie JR, Frampton DM, Mansour PM, Blackburn SI, Nichols PD, Green AG, Singh SP (2007) Isolation and characterization of genes from the marine microalga *Pavlova salina* encoding three front-end desaturases involved in docosahexaenoic acid biosynthesis. Phytochemistry 68:785–796